

Electrochemical Behavior of Bis(cyclopentadienylnickel)–Alkyne Derivatives

Domenico Osella,^{*,1a} Rosanna Rossetti,^{1a} Carlo Nervi,^{1a} Mauro Ravera,^{1a} Marcella Moretta,^{1a} Jan Fiedler,^{1b} Lubomir Pospisil,^{1b} and Edmond Samuel^{1c}

Dipartimento di Chimica IFM, Università di Torino, via P. Giuria 7, 10125 Torino, Italy, The J. Heyrovsky Institute of Physical Chemistry, Academy of Science of the Czech Republic, Dolejskova 3, 182 23 Prague 8, Czech Republic, and Ecole Nationale Supérieure de Chimie, 11 rue P. et M. Curie, 75231 Paris, France

Received April 8, 1996[⊗]

The electrochemical behavior of dimetallic $[\text{Ni}_2\text{Cp}_2](\text{RC}\equiv\text{CR}')$ ($\text{Cp} = \pi$ -cyclopentadienyl; $\text{R} = \text{R}' = \text{Ph}$; COOMe ; $\text{R} = \text{H}$, $\text{R}' = \text{Ph}$; $\text{R} = \text{Me}$, $\text{R}' = \text{Ph}$; $\text{R} = \text{Ph}$, $\text{R}' = -\text{C}\equiv\text{CPh}$) and tetrametallic $\text{M}_2\text{M}_2'(\text{PhC}\equiv\text{CC}\equiv\text{CPh})$ ($\text{M}_2 = \text{M}_2' = \text{Ni}_2\text{Cp}_2$; $\text{M}_2 = \text{Ni}_2\text{Cp}_2$, $\text{M}_2' = \text{Co}_2(\text{CO})_6$) derivatives has been investigated. All dinickel compounds undergo an electrochemically and chemically reversible 1e (metal-centered) reduction followed by further ligand-based reductions. The tetrametallic complex $[\text{Ni}_2\text{Cp}_2]_2(\text{PhC}\equiv\text{CC}\equiv\text{CPh})$ shows two fully reversible 1e (metal-centered) reductions, indicating a strong electronic communication between the two redox units ($\Delta E^\circ = 670$ mV). The mixed-metal $[\text{Ni}_2\text{Cp}_2][\text{Co}_2(\text{CO})_6](\text{PhC}\equiv\text{CC}\equiv\text{CPh})$ derivative exhibits a 1e (Co_2 -centered) reduction at first, followed by a further 1e (Ni_2 -centered) reduction; such an electrochemical scenario is complicated by a fast decomposition following the first reduction, which produces some amount of $[\text{Ni}_2\text{Cp}_2](\text{PhC}\equiv\text{CC}\equiv\text{CPh})$ compound, having a dangling (uncoordinated) triple bond.

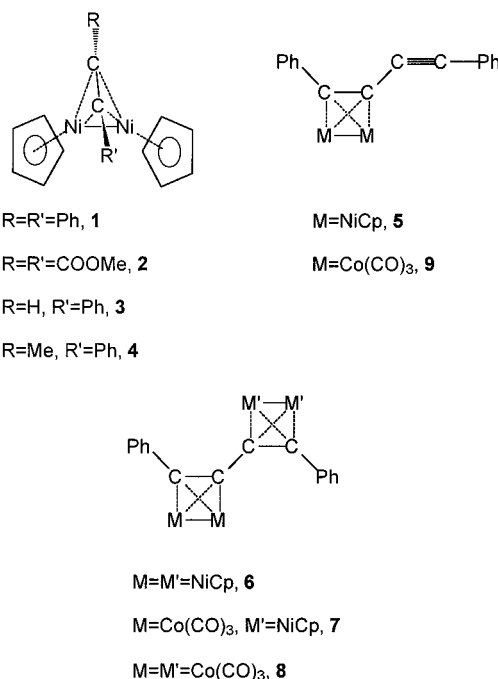
Introduction

While the electrochemical behavior of the $\text{Co}_2(\text{CO})_6$ - (alkyne) series has been elucidated in reasonable detail,² one can find only brief reports on the electrochemical features of the isoelectronic and isostructural Ni_2Cp_2 - (alkyne) derivatives. Dessy *et al.* in their exhaustive investigation on *literally* hundreds of organometallic compounds described a 1e reduction at a very cathodic potential in dimethoxyethane for $\text{Ni}_2\text{Cp}_2(\text{HC}\equiv\text{CH})$ and $\text{Ni}_2\text{Cp}_2(\text{PhC}\equiv\text{CPh})$ complexes;³ additionally, an oxidation is mentioned by Geiger *et al.* for the second derivative.⁴ The isoelectronic diphenylacetylene–dipalladium complex $(\text{C}_5\text{Ph}_5)_2\text{Pd}_2(\text{PhC}\equiv\text{CPh})$ exhibited two oxidation processes and one reduction process.⁵

Results and Discussion

Electrochemistry of Dimetallic Derivatives. The electrochemical responses of all $\text{Ni}_2\text{Cp}_2(\text{RC}\equiv\text{CR}')$ ($\text{R} = \text{R}' = \text{Ph}$, **1**; $\text{R} = \text{R}' = \text{COOMe}$, **2**; $\text{R} = \text{H}$, $\text{R}' = \text{Ph}$, **3**; $\text{R} = \text{Me}$, $\text{R}' = \text{Ph}$, **4**; $\text{R} = \text{Ph}$, $\text{R}' = -\text{C}\equiv\text{CPh}$, **5**) derivatives in tetrahydrofuran (THF) at a Pt electrode are very similar.

Figure 1 shows the cyclic voltammetric (CV) response of a THF solution of **1** at 0.2 V s^{-1} scan rate. An



irreversible oxidation process is observed at $E_p(\text{A}) = +0.65 \text{ V}$. This oxidation quickly alters the surface of the solid electrode and will no longer be discussed. The first reduction process (peak couple B/C) is diffusion-controlled (the plots of i_p vs $\nu^{1/2}$ and the plot of i_p vs concentration of depolarizer are linear through the origin of the axes), electrochemically reversible (the peak-to-peak separation, $\Delta E_p = E_{pa} - E_{pc}$, is 60 mV and the peak width, $\delta E = E_p - E_{p/2}$, is 57 mV, both independent of scan rate in the whole experimentally used range $0.05\text{--}50 \text{ V s}^{-1}$), and chemically reversible

[⊗] Abstract published in *Advance ACS Abstracts*, January 1, 1997.

(1) (a) Università di Torino. (b) The J. Heyrovsky Institute of Physical Chemistry. (c) Ecole Nationale Supérieure de Chimie.

(2) (a) Arewgoda, M.; Rieger, P. H.; Robinson, B. H.; Simpson, J.; Visco, S. J. *J. Am. Chem. Soc.* **1982**, *104*, 5633. (b) Peake, B. M.; Rieger, P. H.; Robinson, B. H.; Simpson, J. *J. Am. Chem. Soc.* **1980**, *102*, 156.

(3) (a) Dessy, R. E.; Stary, F. E.; King, R. B.; Waldrop, M. *J. Am. Chem. Soc.* **1966**, *88*, 471. (b) Dessy, R. E.; Pohl, R. L. *J. Am. Chem. Soc.* **1968**, *90*, 1995.

(4) Geiger, W. E.; Connelly, N. G. *Adv. Organomet. Chem.* **1985**, *24*, 87.

(5) Broadley, K.; Lane, G. A.; Connelly, N. G.; Geiger, W. E. *J. Am. Chem. Soc.* **1983**, *105*, 2486.

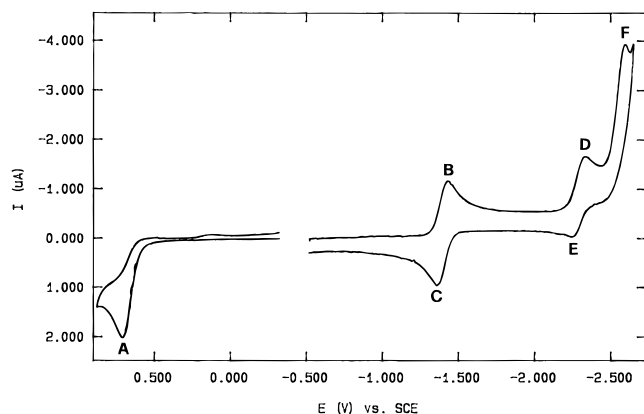


Figure 1. CV response of a THF solution of **1** at a Pt electrode (scan rate 0.2 V s^{-1}).

(the anodic to cathodic peak ratio is unity at each scan rate).⁶ Similar features have been observed for derivatives **2–5** (Table 1). dc polarographic analyses⁶ also show that the plots of E vs $\log(i_d - i)/i$ are linear with slopes of about 60 mV for compounds **1–5** (Table 1). Furthermore, the ac polarographic responses of THF solutions of **1–5** at a dropping mercury electrode (DME) indicate 1e Nernstian behavior: no indication of sluggishness of the electron transfer⁶ has been detected at frequencies as high as 3 kHz (Figure 2). The stoichiometry of the first reduction is confirmed by the height of the peaks (in CV) or the waves (in polarography) when compared with the 1e oxidation process of decamethylferrocene (Fc^*) added as internal standard.⁷ However, in the case of **1**, exhaustive electrolysis at a mercury pool performed at $E_{\text{appl}} = -1.60 \text{ V}$ consumes a very large amount of charge; even after 6 faradays/mol are consumed, the original polarographic reduction wave B is retained almost quantitatively.⁸ Similar behavior is observed by changing the solvent (CH_2Cl_2 in lieu of THF) and the supporting electrolyte (LiClO_4 in place of $[\text{NBu}_4][\text{PF}_6]$) as well as by using a Pt basket as the cathode instead of the mercury pool. Catalytic reductions could be invoked to justify this conflicting evidence, as like in the case of the $[(\pi\text{-C}_5\text{H}_5)\text{Fe}(\text{CO})_4]$ cluster.⁹

Complexes **2–5** show similar coulometric regimes with somewhat smaller stability of the electrogenerated anions during the catalytic cycle.

The further reductions of compounds **1–5** observed at more cathodic potentials closely resemble those of the corresponding free ligands.¹⁰ For instance, the CV response of **1** shows two further peaks at $E_p(\text{D}) = -2.36 \text{ V}$ and at $E_p(\text{F}) = -2.61 \text{ V}$ at 0.2 V s^{-1} (Figure 1), whereas the CV response of $\text{PhC}\equiv\text{CPh}$ under the same experimental conditions exhibits two reduction proc-

esses at peak potentials of -2.34 and -2.62 V , respectively. By using a scan rate higher than 1 V s^{-1} (CV) or a frequency above 64 Hz (ac voltammetry), full chemical reversibility is achieved for the peak couple D/E, giving a formal redox potential of -2.29 V for 1e reduction. The further reduction near the solvent discharge (peak F) remains irreversible on any time scale. In a polarographic test, when CH_3COOH is added to a THF solution of **1** (Figure 3), the Ni_2 -centered wave B remains practically unperturbed while the two further ligand-based reductions (namely wave D and F) collapse into a single wave that is double in height and is shifted toward more positive potential. This behavior is typical of reduction of organic compounds with consumption of protons, such as unsaturated hydrocarbons.¹⁰

Electrochemistry of 6. Figure 4 shows the CV response of a THF solution of $[\text{Ni}_2\text{Cp}_2]_2(\text{PhC}\equiv\text{CC}\equiv\text{CPh})$, (**6**), containing an equimolar amount of Fc^* as an internal standard. Compound **6** exhibits two well-resolved metal-centered 1e reductions at $E^{\prime}(0,0/1-,0) = -1.26 \text{ V}$ (peak couple G/H)¹¹ and $E^{\prime}(1-,0/1-,1-) = -1.93 \text{ V}$ (peak couple I/L). Classical polarographic and CV tests as described above for **1–5** were performed, and they confirmed the 1e reversible character of both reduction processes in **6**. The corresponding ligand-centered reductions are likely shifted behind the solvent discharge. A strong interaction between the two redox-active Ni_2Cp_2 units in **6** is evident, with a ΔE^{\prime} value of 670 mV. From this large potential separation, a high comproportionation constant K_c of 2.1×10^{11} was evaluated.¹² This electronic interaction is significantly larger than that found for the isoelectronic analogue $[\text{Co}_2(\text{CO})_6]_2(\text{PhC}\equiv\text{CC}\equiv\text{CPh})$, (**8**), namely $\Delta E^{\prime} = 350 \text{ mV}$.¹³ In that case the redox process was complicated by subsequent decomposition and we performed CV experiments at subambient temperatures in order to obtain the relevant thermodynamic parameters.¹¹ In addition to the intrinsic stability of electrogenerated anions, a further reason for the stronger electronic communication in **6** with respect to **8** may lie in different structural rearrangements of the diyne, which obviously changes the degree of π -overlapping. While the structure of **8** has been published,¹⁴ several attempts to obtain crystals of **6** suitable for an X-ray determination have been unsuccessful to date.

To obtain some insight into the electronic differences between **6** and **8**, we employed simple EHT calculations (CACAO package).¹⁵ The geometry of the model complex $\text{Co}_2(\text{CO})_6(\text{HC}\equiv\text{CH})$ was built up according to the procedure previously published by Hoffmann et al.¹⁶ Then, after formal removal of an hydrogen atom in each structure, the two fragments $\text{Co}_2(\text{CO})_6(\text{HC}\equiv\text{C}-)$ were linked, imposing a C–C distance of 1.430 \AA ¹⁴ and an overall C_{2h} symmetry. The structure of the model

(6) (a) Bard, A. J.; Faulkner, L. R. *Electrochemical Methods*; Wiley: New York, 1980. (b) Kissinger, P. T.; Heineman, W. R. *Laboratory Techniques in Electroanalytical Chemistry*; Dekker: New York, 1984. (c) Galus, Z. *Fundamentals of Electrochemical Analysis*; Ellis Horwood: Chichester, U.K., 1994. (d) Delahay, P. *New Instrumental Methods in Electrochemistry*; Interscience: New York, 1954.

(7) Decamethylferrocene (Fc^*) was used as an internal standard instead of ferrocene (Fc), since the oxidation wave of the latter interferes with those of Ni_2Cp_2 (alkyne) derivatives.

(8) Possible reduction of adventitious oxygen has been excluded by performing a coulometric test under the same experimental conditions on the $\text{Co}_2(\text{CO})_6\text{C-Ph}$ cluster, which showed the consumption of 1 faraday/mol, as expected.

(9) Ferguson, J. A.; Meyer, T. J. *J. Am. Chem. Soc.* **1972**, *94*, 3409.

(10) Kiesele, H.; Heinze, J. In *Organic Electrochemistry*; Lund, H., Baizer, M. M., Eds.; Dekker: New York, 1991; p 331.

(11) It is generally accepted that a redox process becomes energetically more favorable as the degree of interaction and the number of sites increase.¹² In the actual case, one can observe that the first reduction of **6** roughly corresponds with the sole metal-centered reduction of **5**. The addition of a second Ni_2Cp_2 moiety as one goes from **5** to **6** (having an electron-donating character) likely compensates the aforementioned stabilizing effect.

(12) Ward, M. D. *Chem. Rev.* **1995**, *24*, 121 and references therein.

(13) Osella, D.; Milone, L.; Nervi, C.; Ravera, M. *J. Organomet. Chem.* **1995**, *488*, 1.

(14) Johnson, B. F. G.; Lewis, J.; Raithby, P. R.; Wilkinson, D. A. *J. Organomet. Chem.* **1991**, *408*, C9.

(15) Mealli, C.; Proserpio, D. M. *J. Chem. Educ.* **1990**, *67*, 399.

(16) Hoffman, D. M.; Hoffmann, R.; Fisel, C. R. *J. Am. Chem. Soc.* **1982**, *104*, 3858.

Table 1. Metal-Centered Redox Potentials (V vs SCE) of Compounds 1–7

compd	CV, Pt working electrode			dc polarography		ac polarography	
	$E_p(0/1+)$	$E''(0,1-)^a$	$E'(0,1-/1-,1-)^a$	$E_{1/2}(0/1-)$	slope (mV)	$E_{su}(0/1-)^b$	$W_{1/2}$ (mV)
1	+0.65	-1.40		-1.40	63	-1.40	92
2	+1.13	-1.01		-1.00	59	-1.03	92
3	+0.65	-1.46		-1.48	60	-1.46	93
4	+0.40	-1.85		-1.83	59	-1.86	92
5	+0.77	-1.26		-1.25	60	-1.27	91
6		-1.26	1.93				
7	+0.79 ^c	-0.95 ^c	-1.62 ^c				

^a Evaluated as $(E_p^\circ + E_p^a)/2$. ^b The term summit potential has been suggested by the IUPAC commission of Electroanalytical Chemistry.²⁶ ^c Measured at -60 °C.

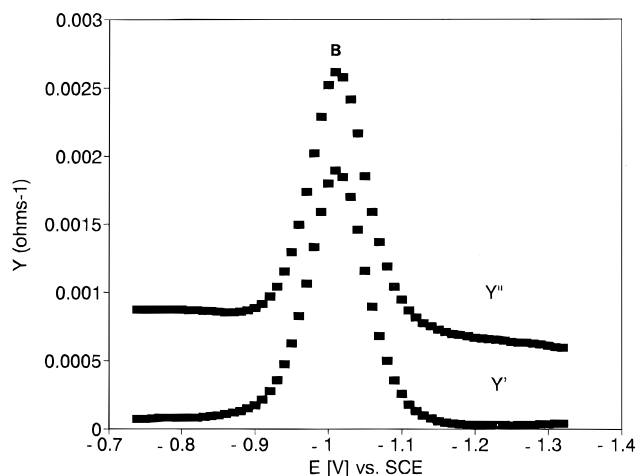


Figure 2. ac polarographic response of a THF solution of **4** at a DME electrode (frequency 3.0 kHz). Y' represents the in-phase component and Y'' the quadrature components of the electrode admittance.

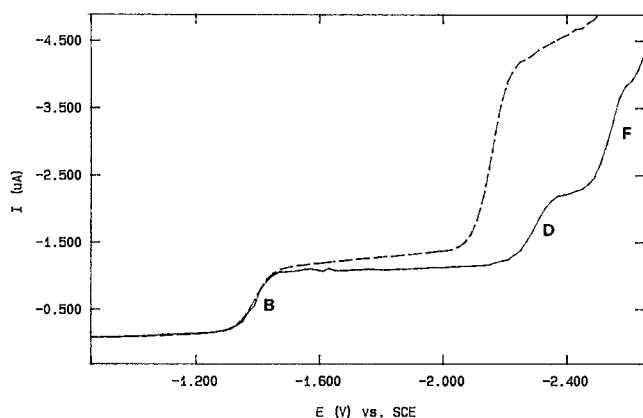


Figure 3. Sampled dc polarographic response of a THF solution of **1** at a DME electrode before (solid line) and after (dashed line) addition of CH_3COOH in the molar ratio 2:1.

$[\text{Co}_2(\text{CO})_6]_2(\text{HC}\equiv\text{CC}\equiv\text{CH})$ turned out to be very similar to that experimentally found for **8**.¹⁴ The same procedure was repeated by starting from the known structure of $\text{Ni}_2\text{Cp}_2(\text{HC}\equiv\text{CH})$,¹⁷ giving rise to the model $[\text{Ni}_2\text{Cp}_2]_2(\text{HC}\equiv\text{CC}\equiv\text{CH})$ (Figure 5). In both models, the LUMO's composition is mainly metal–metal antibonding in character with partial contribution (ca. 10%) of the butadiyne π -orbitals. In the case of the Ni_4 model, there is, however, a significant contribution of ancillary Cp ligands (ca. 20%), suggesting possible delocalization of the extra electron in the corresponding monoanion.

ESR Studies. Unfortunately, the exhaustive electrolysis of **6** shows the same catalytic features as **1**;

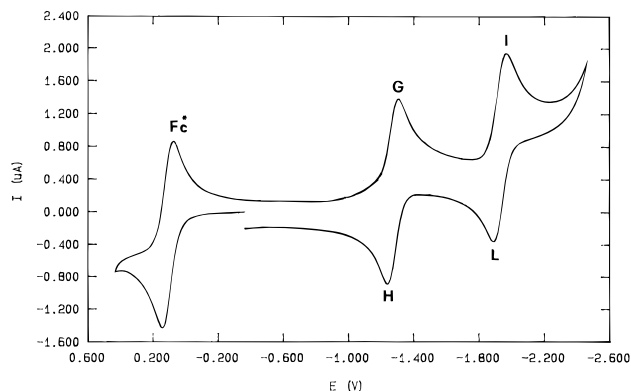


Figure 4. CV response of THF solutions of equimolar samples of **6** and decamethylferrocene (Fc^*) at a Pt electrode (scan rate 0.2 V s^{-1}).

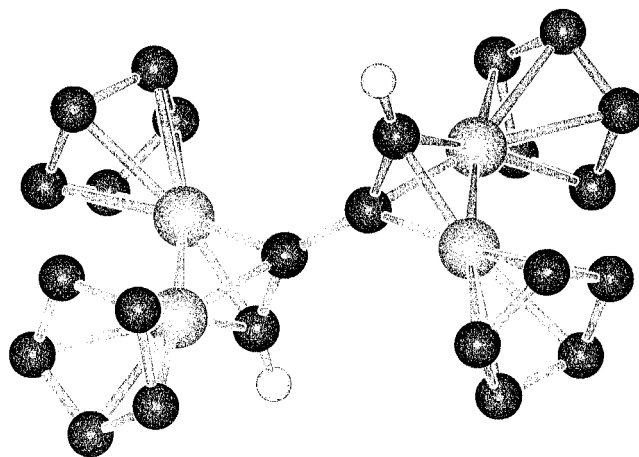


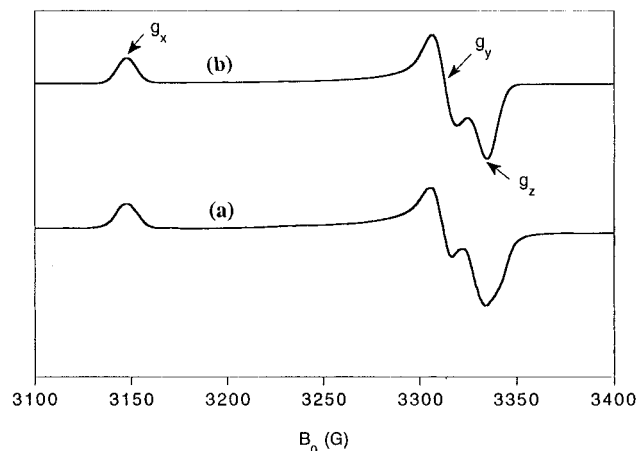
Figure 5. SCHAKAL plot of the structure of the model compound $[\text{Ni}_2\text{Cp}_2]_2(\text{HC}\equiv\text{CC}\equiv\text{CH})$.

therefore, we were not able to produce quantitatively $\mathbf{6}^-$ and $\mathbf{6}^{2-}$ by controlled-potential coulometry. In an attempt to gain further insight into the nature of the reduced species, we selected the three representative compounds **1**, **5**, and **6** and submitted them to investigation using a variable-temperature ESR/galvanostatic electrochemical cell for the detection in situ of radicals inside the cavity of the ESR spectrometer. Application of reductive current at room temperature for a few seconds generated in all three cases a signal of moderate intensity composed of a singlet without other additional features. Performing the electrolysis at low temperatures down to 220 K resulted only in progressive band broadening ($\Delta B = 6.5, 9.7,$ and 28.0 G at 273 K and $\Delta B = 11.3, 16.2,$ and 40.0 G at 223 K for **1**, **5**, and **6**, respectively; $1 \text{ G} = 0.1 \text{ mT}$), the g values remaining constant over this temperature range. The increasing bandwidth at a given temperature as one goes from **1**

Table 2. EPR Parameters of Compounds **1**⁻, **5**⁻, and **6**⁻ in Liquid and Frozen Solutions

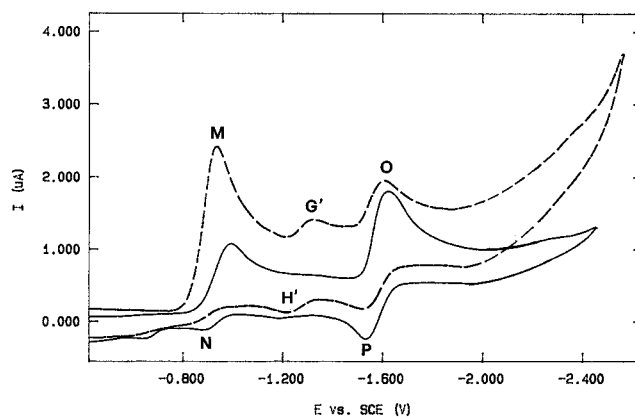
compd	g_{\parallel}	g_{\perp}	g_{iso}
1 ^{-a}	2.115	2.025	2.054
1 ^{-b}	2.114	2.025	2.055
5 ^{-a}	2.115	2.020	2.052
6 ^{-a}	2.125	2.019	2.045 ^c
		2.005	2.050 ^d

^a Generated by electrochemical reduction. ^b Generated by reduction with Na metal. ^c Measured. ^d Computer simulation using $\Delta B = 10$ G (Gaussian). $g_{\parallel} = g_x$, $g_{\perp} = g_y, g_z$

**Figure 6.** Experimental (a) and simulated (b) frozen-solution spectra of electrochemically reduced $[(Cp_2Ni_2)_2(PhC\equiv CC\equiv CPh)]$ (**6**) at 140 K (frequency 9.3621 GHz).

to **6** and progressive band broadening as the temperature is lowered can be correlated with increasing molecular volume and incomplete averaging of the g tensor due to the tumbling motion. At 140 K, the frozen solutions gave well-resolved anisotropic spectra indicative of axial symmetry for **1** and **5**. For **6** a small splitting of the perpendicular component was observed, and computer simulation using the parameters in Table 2 gave a satisfactory replica of the experimental spectrum.

The g values of the frozen-solution spectra for all three compounds are consistent with the structure of a d^9 Ni complex having an unpaired electron residing in a $d(x^2 - y^2)$ or a $d(xy)$ orbital on a single Ni site in the molecule. The measured isotropic g values in the liquid solution are rigorously the same values calculated from the relation $g_{av} = 1/3(g_{\parallel} + 2g_{\perp})$ for **1** and **5**, so that the ESR results are in agreement with single-electron transfer as deduced from CV and ac polarographic measurements. However, some discrepancy was observed for **6** using the relation $1/3(g_x + g_y + g_z)$, which gave a g_{av} value slightly different from the measured one, as shown in Table 2. This could arise from a difference in the interaction modes of the unpaired electron within the radical complex in the fluid and the frozen solutions. It can be reasonably admitted that, for this compound, the unpaired electron in the mono-anion is delocalized over two nonequivalent thermally accessible Ni sites. The isotropic g values of these two sites being slightly different, the broad singlet observed could be due to the sum of two signals centered on two slightly different fields. At 140 K the unpaired electron is trapped on a single site, giving the observed frozen-solution spectrum relative to a single metal site. It should be mentioned that chemical reduction with

**Figure 7.** CV response of a THF solution of **7** at a Pt electrode (scan rate 0.2 V s^{-1}) at room temperature (dashed line) and at $-20 \text{ }^\circ\text{C}$ (solid line).

sodium metal in THF gave ESR spectra having parameters identical with those observed by electrochemical reduction.

These results show that in all cases the only paramagnetic product detected is that of a metal radical with the electron residing on a single Ni site. No additional information can be obtained because of the low percentage of Ni isotopes with a magnetic moment (^{61}Ni , $I = 3/2$, natural abundance 1.19%), which prevents resolution of the hyperfine interaction with the Ni nuclear spin; therefore, some valuable information is lost. It should be mentioned that, to our knowledge, not many data are known for the ESR of paramagnetic Ni compounds.¹⁸

Electrochemistry of 7. The CV response of a THF solution of the mixed-metal derivative $[Ni_2Cp_2][Co_2(CO)_6](PhC\equiv CC\equiv CPh)$, (**7**) exhibits two main couples, M/N and O/P, respectively (Figure 7). The first reduction is chemically irreversible at room temperature; it is likely localized on the $Co_2(CO)_6$ center, as one can deduce from its reduction potential. The second reduction is chemically reversible, and we assign it to the reduction of Ni_2Cp_2 unit by the same reasoning. At room temperature, the smaller peak couple G'/H' can be observed, whose potential corresponds to that of "dangling" derivative **5**. When the temperature is lowered to $-20 \text{ }^\circ\text{C}$, couple M/N becomes partially reversible, while couple G'/H' disappears (Figure 7). A cyclic voltammogram with switching potential at -1.20 V (after the first reduction) yields the completely reversible redox pair M/N. We interpret this puzzle (Figure 8) by assuming the occurrence of an ECE mechanism at room temperature: part of the mono-anion **7**⁻ decomposes, forming **5**, which is further reduced at peak G' . The formation of **5** has been verified after exhaustive electrolysis by TLC comparison with an authentic sample of **5**. Increasing the scan rate up to 10 V s^{-1} causes this reaction to be suppressed, and complete reduction of **7**⁻ to **7**²⁻ takes place at peak couple O/P. This scheme resembles the decomposition of $[Co_2(CO)_6]_2(PhC\equiv CC\equiv CPh)$ (**8**) to $[Co_2(CO)_6](PhC\equiv CC\equiv CPh)$, (**9**), previously demonstrated by electrochemical simulation.¹³

(18) (a) Bowmaker, G. A.; Boyd, P. D. W.; Campbell, G. K.; Hope, J. M.; Martin, R. L. *Inorg. Chem.* **1982**, *21*, 1152 and references therein. (b) Geiger, W. A.; Rieger, P. H.; Corbato, C.; Edwin, J.; Fonseca, E.; Lane, G. A.; Mevs, G. M. *J. Am. Chem. Soc.* **1993**, *115*, 2314. (c) Kölle, U.; Tingh-Zhen, T.; Keller, H.; Ramakrishna, B. L.; Raabe, E.; Krüger, K.; Raabe, G.; Fleischhauer, J. *Chem. Ber.* **1990**, *123*, 227.

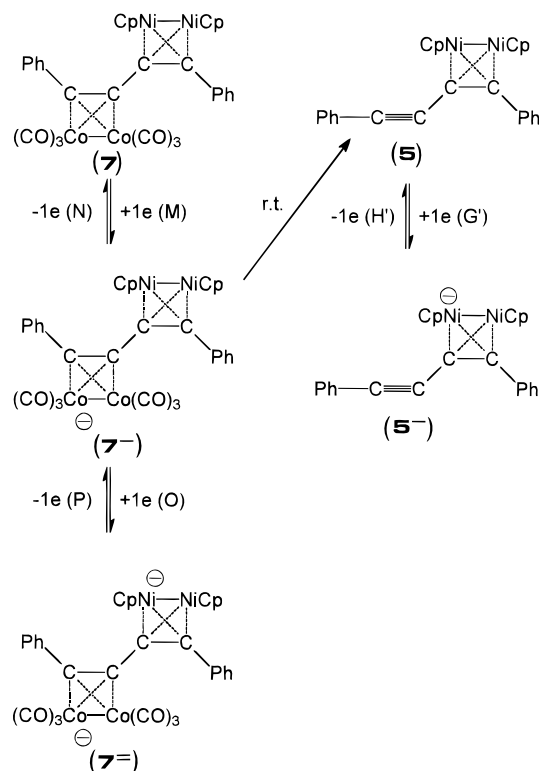


Figure 8. Proposed mechanism for the reduction of **7**.

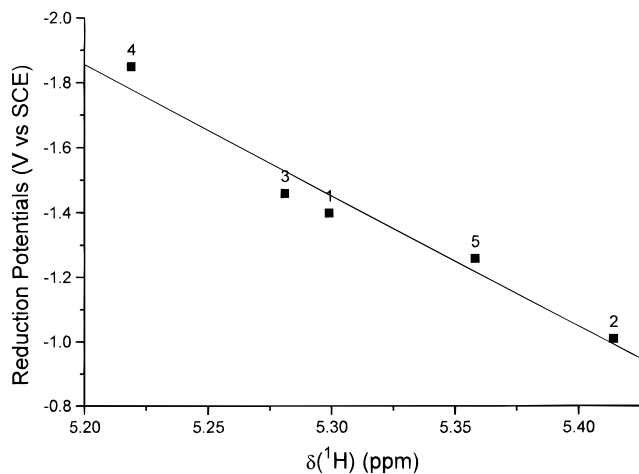


Figure 9. Plot of the metal-centered reduction potentials of compounds **1–5** vs $\delta(^1\text{H})$ of the corresponding cyclopentadienyl ligands. The least-squares slope is 4.04 V/ppm and the correlation coefficient 0.98.

The comparison of the potential of the Co_2 -centered reduction of $\text{Co}_2(\text{CO})_6(\text{PhC}\equiv\text{CC}\equiv\text{CPh})$ (**9**), namely $E^\circ(0/1^-) = -0.87$ V, and the potential of the second Ni_2 -centered reduction of $[\text{Ni}_2\text{Cp}_2]_2(\text{PhC}\equiv\text{CC}\equiv\text{CPh})$ (**6**), namely $E^\circ(0,1^-/1^-,1^-) = -1.93$ V, with those of the first reduction (-0.95 V) and the second reduction (-1.62 V) of **7**, respectively, indicates that the fragment $\text{Co}_2(\text{CO})_6$ acts through the butadiyne chain as an electron-withdrawing substituent, while the fragment Ni_2Cp_2 acts as an electron-donating substituent. This agrees with the trend previously found in $\text{Co}_3(\text{CO})_9(\text{CR})$ clusters by Robinson et al.¹⁹ Furthermore, the shift of the totally symmetric ν_{CO} band²⁰ at lower wavenumbers of the tetrahedral $\text{Co}_2(\text{CO})_6(\text{C}\equiv\text{C})$ moiety as one goes

(19) Colbran, S. B.; Robinson, B. H.; Simpson, J. *Organometallics* **1984**, *3*, 1344.

from **9** to **7** confirms the electron-releasing properties of the Ni_2Cp_2 fragment.

Finally, it was suggested that a linear free energy relationship exists between electronic properties of the acetylene substituents and the $\delta(^1\text{H})$ values of the coordinated Cp.²¹ In fact, any increase of electron density on the metal core should raise the π -electron density of Cp ligands and hence their shielding. We were able to verify this by plotting the Ni_2 -centered reduction potentials of compounds **1–5** (which are a direct measure of the electronic density of the Ni_2 core) against the $\delta(^1\text{H})$ values of the corresponding Cp ligands; a straight line is indeed observed, as shown in Figure 9.

Experimental Section

Compounds **1–4**²¹ and **5–7**²² were synthesized according to published procedures. Their purity was checked by means of microanalysis and ^1H -NMR spectroscopy. For derivatives **5–7**, we report their spectroscopic data, since in the previous publication²² they were characterized only on the basis of their elemental analyses. The IR and ^1H (400 MHz) and ^{13}C NMR (100.577 MHz) spectra were recorded on a Perkin-Elmer 580 B and a JEOL EX 400 instrument, respectively. Desorption chemical ionization (DCI) mass spectra were recorded on a Finnigan-MAT 95Q instrument. 2-Methylpropane was used as the reagent gas at 0.5 mbar pressure. The ion source temperature was kept at 50 °C, the electron emission current at 0.2 mA, and the electron energy at 200 eV. Positive ion spectra were recorded.

5: ^1H NMR (CDCl_3) δ (ppm) 7.7–7.3 (m, 10H, Ph), 5.34 (s, 10H, Cp); ^{13}C NMR (CDCl_3) δ (ppm) 137.83–124.18 (Ph), 99.27, 97.76 (coordinated C_{ac}), 88.04 (Cp), 87.15, 71.82 (uncoordinated C_{ac}); DCI-MS $[\text{M} + \text{H}]^+$ m/z 449 (for ^{58}Ni).

6: ^1H NMR (CDCl_3) δ (ppm) 8.0–7.4 (m, 10H, Ph), 5.20 (s, 20H, Cp); ^{13}C NMR (CDCl_3) δ (ppm) 139.41–127.93 (Ph), 99.62, 90.31 (C_{ac}), 87.61 (Cp); DCI-MS $[\text{M} + \text{H}]^+$ m/z 695 (for ^{58}Ni).

7: ^1H NMR (CDCl_3) δ (ppm) 7.8–7.2 (m, 10H, Ph), 5.24 (s, 10H, Cp); ^1H NMR (CDCl_3) δ (ppm) 198.60 (Co–CO), 139.03–127.11 (Ph), 99.71, 99.32, 92.65, 90.14 (C_{ac}), 88.02 (Cp); IR (*n*-hexane) ν_{CO} 2087 s, 2053 vs, 2028 vs, 2023 sh, 2010 w cm^{-1} ; DCI-MS $[\text{M} + \text{H}]^+$ m/z 735 (for ^{58}Ni).

Electrochemical measurements were performed by using EG&G PAR 273 or EG&G PAR 263 electrochemical analyzers interfaced to personal computers together with, for ac measurements, an EG&G PAR Model 5210 lock-in amplifier employing PAR M270 electrochemical software. A standard three-electrode cell was constructed such that it allowed the tip of the reference system to approach the working electrode closely. An aqueous saturated calomel electrode (SCE) (separated from the cell solution with a Luggin probe) was the operational reference electrode, and all potentials are referred to SCE. The stability of the reference electrode, was verified by frequent measurements of the potential of the reversible $\text{Fc}^*(0/1^+)$ couple, taken as $E^\circ = +0.11$ V by comparison with the $\text{Fc}(0/1^+)$ couple,²³ recorded under the same experimental conditions ($E^\circ = +0.56$ V vs SCE in THF).²⁴ For CV, the working electrode was a platinum disk (diameter 0.1 cm) sealed in Teflon. For polarography, a dropping mercury electrode (DME) was employed; the flow rate was 1.22 mg s^{-1} and the reservoir height 0.5 m. The drop time (typically 1 s)

(20) Palyi, G.; Piacenti, F.; Markó, L. *Inorg. Chim. Acta Rev.* **1970**, *4*, 109.

(21) Randall, E. W.; Rosenberg, E.; Milone, L.; Rossetti, R. Stanghellini, P. L. *J. Organomet. Chem.* **1974**, *64*, 271.

(22) Tilney-Bassett, J. F. *J. Chem. Soc.* **1961**, 577.

(23) Külle, U.; Khouzami, F. *Angew. Chem., Int. Ed. Engl.* **1980**, *19*, 640.

(24) Geiger, W. E. *Organometallic Radical Processes*; Troglor, W. C., Ed.; Elsevier: Amsterdam, 1990; p 144.

was controlled by an electromechanical hammer. Positive-feedback iR compensation was applied routinely.

The remaining uncompensated part of the cell resistance was determined by measurement of the impedance spectrum and by extrapolation of the Z' vs Z'' plot (Nyquist plot) to high frequencies.²⁵ The ac polarographic data were always recalculated-corrected for uncompensated resistance.

All measurements were carried out under Ar in anhydrous deoxygenated THF, distilled from a solution containing sodium benzophenone. Tetrabutylammonium hexafluorophosphate ($[\text{NBu}_4][\text{PF}_6]$) was employed as supporting electrolyte (0.1 M). The temperature of the solutions was kept constant to ± 1 °C

(25) De Levie, R.; Pospisil, L. *J. Electroanal. Chem.* **1969**, *22*, 277.

(26) Meites, L.; Zuman, P.; Nurberg, H. W. *Pure Appl. Chem.* **1985**, *57*, 1491.

by circulation of a thermostated water-ethanol mixture through the double wall of the cell.

ESR spectra were performed with a Bruker ER-10 spectrometer using dpph (2,2'-diphenylpicrylhydrazyl) as reference standard.

Acknowledgment. We thank the European Union (EU, Brussels, Belgium; Contracts ERBCIPAACT922266 and ERBCIPAACT930027) and the Czech Ministry of Education (Praha, Czech Republic) for financial support. We are grateful to the reviewers for their perceptive comments.

OM960270J